bioRxiv preprint doi: https://doi.org/10.1101/011320; this version posted November 12, 2014. The copyright holder for this preprint (which was not certified by peer review) is the author/funder. All rights reserved. No reuse allowed without permission.

Wide field-of-view, twin-region two-photon imaging across extended cortical networks

Jeffrey N. Stirman[1,2], Ikuko T. Smith[1,5], Michael W. Kudenov[6], and Spencer L. Smith[1-4]

[1] Neuroscience Center
[2] Carolina Institute for Developmental Disabilities
[3] Department of Cell Biology and Physiology
[4] Neurobiology Curriculum
[5] Department of Pharmacology
[6] Department of Electrical and Computer Engineering, North Carolina State University

University of North Carolina School of Medicine, Chapel Hill, NC 27599

Correspondence should be addressed to
slab@unc.edu (S.L.S.)

bioRxiv preprint doi: https://doi.org/10.1101/011320; this version posted November 12, 2014. The copyright holder for this preprint (which was not certified by peer review) is the author/funder. All rights reserved. No reuse allowed without permission.

Two-photon calcium imaging can provide an optical readout of spiking activity with cellular resolution, revealing activity correlations and population dynamics within an individual cortical area. However, many conventional two-photon imaging systems maintain cellular resolution only over a field of view (FOV) ~500 µm wide. This FOV precludes the simultaneous visualization of multiple cortical areas, which can be spread over a millimeter or more. Thus it has not typically been possible to use two-photon calcium imaging to measure neural activity dynamics and correlations between cortical areas. Here, we demonstrate a new two-photon imaging system that is designed to image neural activity in multiple cortical areas simultaneously. Low aberration scan optics support an expanded FOV with cellular resolution that is 1.4 to 1.8 mm wide using a commercially available objective, and 3.5 mm wide using a custom objective. Two independently positionable multiplexed excitation pathways simultaneously image any two regions within the expanded FOV. We use this new imaging system to measure activity correlations between two cortical visual areas in mice.

Ensemble neuronal activity is of key interest in system neuroscience to understand sensory coding, motor output, and cognitive function. Measuring neuronal activity in populations of neurons *in vivo* is technically challenging, due to the densely packed neuropil and sensitive neuroanatomy that is best probed with minimally invasive approaches. Two-photon[1] population calcium imaging *in vivo*[2] offers many distinct advantages over alternative approaches such as metal electrodes. Two-photon calcium imaging provides unambiguous identification of recorded neurons, particularly when genetically encoded indicators are employed[3]. It can be used to record activity in tens to hundreds of neurons by imaging somata, dendrites, or axons in local populations[4-10]. Furthermore, two-photon imaging can image deep in scattering tissue, for example hundreds of microns into mammalian neocortex[11,12]. Not only has this approach revealed cellular-level stimulus selectivity in dense local ensembles of neurons[6,13], but it can be used to measure neural activity in awake mice performing a psychophysics task[8], or navigating in a virtual reality environment[14].

Although two-photon imaging has proven to be a powerful tool to study ensemble activity in local populations of neurons in neocortex, conventional approaches are limited to a full field of view (FOV) of that is approximately 500 µm wide. This limitation largely precludes the simultaneous examination of multiple cortical areas. The discrete functional areas of mammalian neocortex work in concert to process sensory input and guide adaptive behavior. However, we know little about how cortical areas interact. Thus progress in systems neuroscience requires a cellular-level view into ongoing neural activity across extended cortical networks.

Here we present a new two-photon imaging system that features a wide field of view and two imaging beams that are synchronously scanned, enabling simultaneous two-photon calcium imaging in spatially separate cortical areas. We have named the system the Trepan2p (Twin Region, Panoramic 2-photon) microscope.

RESULTS

Cortical networks in the mouse visual system (primary visual cortex, V1, and several higher visual areas, HVAs) can extend across millimeters of neocortex[15]. Conventional two-photon imaging systems have FOVs that largely preclude imaging multiple cortical areas (**Fig. 1a**). The development of the Trepan2p was motivated by two experimental needs: (1) the ability to image extended cortical networks, which requires increasing the overall FOV to > 1 mm, and (2) the ability to simultaneously image two regions of interest (ROIs) within an expanded FOV, to capture synchronous dynamics of neural activity across extended cortical networks with relevant temporal resolution. To address these needs, the Trepan2p microscope embodies two major advances. First, it can image a FOV of 1.4 mm (**Fig. 1b)** to 3.5 mm across depending on the objective used. This represents a 7 to 50-fold increase in imaging area compared to conventional two-photon microscopes. Second, within this large FOV, any two areas can be simultaneously imaged (**Fig. 1c**) with multiplexed imaging beams, capturing cortical dynamics across extended networks with cellular and subcellular resolution with higher temporal resolution.

Scanning laser beams across a large FOV while maintaining high efficiency excitation presents challenges that are not well addressed by conventional two-photon imaging optics. Chiefly, optical aberrations occur at high scan angles that greatly degrade the focus of the excitation spot and result in poor efficiency of two-photon excitation. In many conventional two-photon microscopes, the *X* and *Y* galvanometer scanners are placed close together. This arrangement is acceptable when scan angles are small, and simplifies the optical layout. However, when scan angles are large (e.g., to obtain a wide FOV; **Fig. 1b**) the deflection from the first scan mirror causes part of the beam to miss the second scan mirror, and thus causes a significant decrease in excitation energy and efficiency. To prevent this, an afocal pupil relay between the two galvanometer scanners can be used[16]. While this improves imaging at large scan angles, simple lens systems (e.g., single element aspherical, spherical, or cemented achromatic lenses) cause third order astigmatism that ultimately limits the performance. These aberrations lead to highly inefficient two-photon excitation due to a severely distorted focal spot, and unusable image quality outside a ~500 µm wide FOV. Our design improves the relay system and decreases the oblique astigmatism introduced by large scan angles. For this, we used a compound lens system consisting of 25 mm aspheric lenses (Edmund Optics) and 100 mm positive meniscus lenses (Thorlabs) with the convex surfaces facing each other. These compound lenses have relatively short focal lengths and high NAs to allow for large deflections, and minimize the

bioRxiv preprint doi: https://doi.org/10.1101/011320; this version posted November 12, 2014. The copyright holder for this preprint (which was not certified by peer review) is the author/funder. All rights reserved. No reuse allowed without permission.

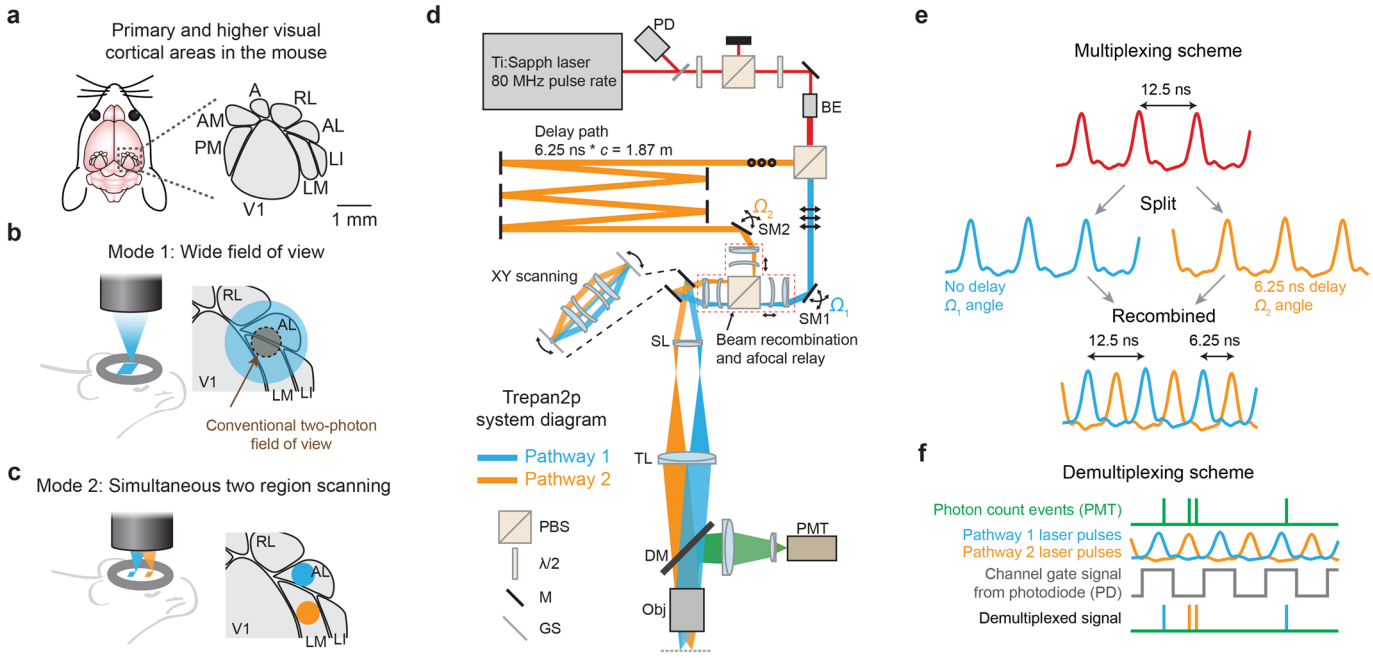

Figure 1. Motivation and design of the Trepan2p microscope. (a) In mice, primary visual cortex (V1) is surrounded by higher visual areas (PM, AM, A, RL, AL, LM, and LI). **(b)** To examine activity in multiple cortical areas, it is necessary to have a large field of view. Conventional two-photon imaging is limited to narrow border regions that fail to cover significant portions of mouse cortical areas. By contrast, a expanded field-of-view (FOV) would cover more cortical area and enable investigations of activity in multiple cortical areas. **(c)** Raster scanning a large FOV is necessarily slow compared to scanning a small FOV. Thus, depending on the experiment goals, it would be ideal to have two imaging beams that can act like movable spotlights across the field of view. **(d)** Laser pulses detected by a photodiode (PD) using a pick-off mirror. This signal is used for demultiplexing later, as shown in (f). Power is attenuated using a half-wave plate (λ/2) and a polarizing beam splitting cube (PBS). After a second λ/2 (used to determine the power ratio sent to the two pathways) and a beam expander (BE), a second PBS divides the beam into two pathways. Pathway 1 (in blue, p-polarization, indicated by the arrows) passes directly to a steering mirror (SM1). Pathway 2 (in orange, the s-polarization, indicated by the circles), passes to a delay arm where it travels 1.87 meters further than pathway 1, thus delaying it by 6.25 ns. Then Pathway 2 is directed to SM2. The two pathways are recombined using an afocal relay and a third PBS (**SI Fig. 1d-f**), and the beam is relayed to *X* and *Y* galvanometer scanners that are connected by an afocal relay (expanded view inset; **SI Fig. 1a-c**). A scan lens and tube lens focus the two multiplexed beams onto the back aperture of the objective. Fluorescence is directed to a photomultiplier tube (PMT) via an infrared-passing dichroic mirror (DM). **(e)** In the multiplexing scheme, laser pulses are split into two pathways, and pathway 2 is delayed. The 6.25 ns delay in pathway 2 results in perfectly interleaved pulses upon recombination. Both pathways have different deflection angles (Ω_1 or Ω_2) on the galvanometer scanning mirrors, as dictated by SM1 and SM2. **(f)** The signals from the two pathways are demultiplexed using synchronization pulses from the photodiode (PD, shown in panel d). Pulses from the PMT are detected by fast photon counting electronics, and are assigned to be from one of the two pathways, depending on the state of the gating signal.

mechanical space occupied. The compound lens relay exhibited reduced astigmatism compared to a simple lens relay (**SI Fig. 1a-c**), enabling improved two-photon excitation across larger scan angles to support expanded FOVs.

In the Trepan2p microscope, two imaging pathways (Mode 2, **Fig. 1c**) are established using temporal multiplexing[17,18]. Laser pulses from a Ti:Sapphire laser (Mai-Tai, Spectra Physics/Newport) are attenuated and split into two beams using two sets of polarization optics (**Fig. 1d**). One beam travels directly to a custom motorized steering mirror, and the other beam is first diverted to a delay arm, and subsequently to a separately controlled steering mirror (**Fig. 1d**). The delay arm is designed to impart a 6.25 ns delay to the pulses in one beam (1.875 m additional path length). Since the laser pulses are delivered at 12.5 ns intervals (80 MHz), they are evenly spaced in time at 160 MHz after the two beams are recombined with a third polarization cube (**Fig. 1d,e**).

The steering mirror in each pathway imparts a solid angle (Ω_1 or Ω_2) deflection to the beam prior to recombination (**Fig. 1d**). It is these angles that determine the central locations (X_1, Y_1; X_2, Y_2) of individual ROIs within the larger FOV. The two beams are recombined and relayed to the *X*-axis galvanometer scanner using the third polarization cube located in the middle of an afocal pupil relay, in which aberrations are reduced using the same principles as used in the relay between the *X* and *Y* galvanometer scanners. In this manner the two beams are simultaneously raster scanned (field size determined by scan amplitude), but with independently controlled spatial positions (determined by Ω_1, Ω_2). For the afocal relay, to accommodate the path length occupied by the polarizing beam cube, we used a 50 mm achromatic lens (Thorlabs) in

bioRxiv preprint doi: https://doi.org/10.1101/011320; this version posted November 12, 2014. The copyright holder for this preprint (which was not certified by peer review) is the author/funder. All rights reserved. No reuse allowed without permission.

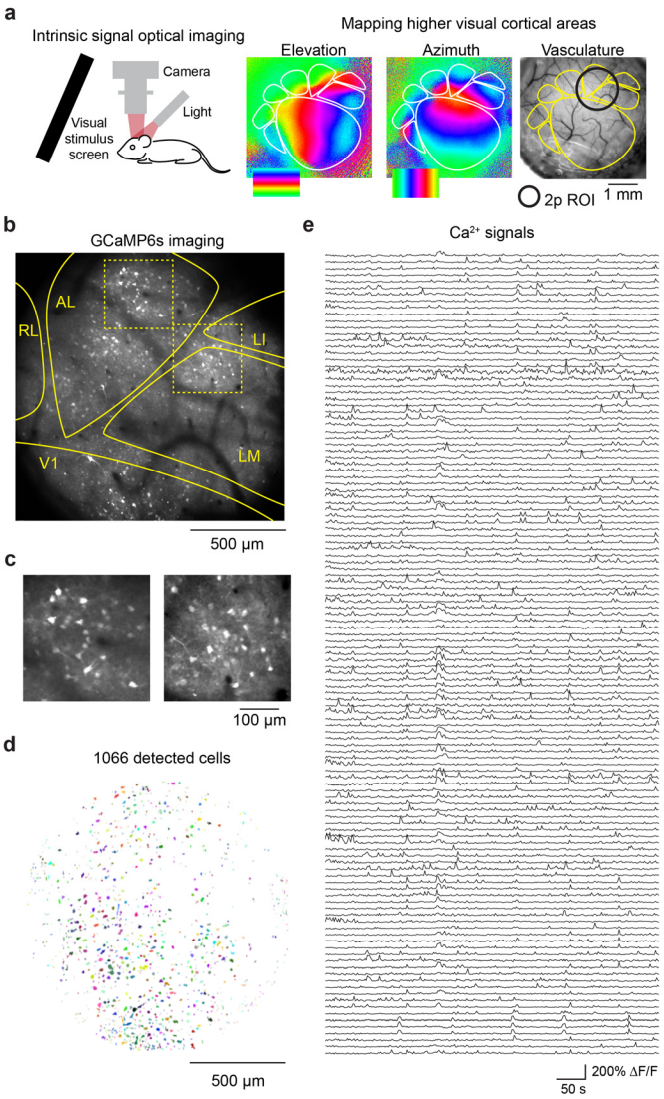

Figure 2. Two-photon calcium imaging across a 1.4 mm wide field of view. (a) Visual cortical areas of the mouse were mapped using intrinsic signal optical imaging (see **Online Methods** for stimulus and protocol). Maps of elevation and azimuth retinotopy revealed meridians that form the borders between cortical areas. These maps were superimposed on maps of vasculature for later registration with two photon images. **(b)** A GCaMP6s-expressing mouse was used to simultaneously image a majority of area AL, about half of area LM, and portions of V1, RL, and LI. **(c)** Expanded view of images of the boxed regions in panel b. Cellular and subcellular resolution was preserved in this imaging mode. **(d)** Over 1000 cells were detected across this single plane field of view. **(e)** High fidelity Ca^{2+} signals were detected across the entire field of view.

combination with a 100 mm positive meniscus lens (Edmund Optics) with the convex surface of the meniscus facing the crown glass of the achromatic lens. Again, this led to a great reduction in aberrations (**SI Fig. 1d-f**) allowing for large angles ($\Omega_1, \Omega_2 \neq 0$) to be imparted on the individual imaging pathways. Additionally, axial movement of the meniscus lens causes a small change in beam convergence that can alter the focal plane for that particular path. Alternatively, we could use a tunable lens[19] placed close to the afocal relay entrance pupil position. This would give a greater degree of axial travel. Therefore, each path is fully independently positionable in *X, Y,* and *Z*.

A scan lens and tube lens form a 4x telescope, relaying an expanded beam to the back aperture of the objective (12.5 mm focal length, 0.8 NA, Nikon; 16 x magnification in this configuration). Overall, the system transmitted ~13% of entering laser power. The main factors influencing this figure were the galvanometer scanners and objective, which were both overfilled (accounting for ~69% of total power loss). The system was not power limited in this configuration.

Fluorescence was collected using a dichroic mirror, two lenses[20], and a GaAsP photomultiplier tube (PMT; H10769PA-40, Hamamatsu) with a high bandwidth amplifier (C5594-44, Hamamatsu). A photodiode (DET02AFC, Thorlabs) was used to detect laser pulses and synchronize photon-counting electronics. A gated fluorescence lifetime photon-counting unit (PMS-400A, Becker & Hickl) was repurposed for this application and obviated the need for custom electronics. By synchronizing the photon counting electronics (PMS-400A) with the laser pulses, fluorescence events can be reliably assigned to the appropriate pathway (**Fig. 1f**) with minimal channel crosstalk (1.5 – 6.6%; **SI Fig. 2**). Photon counting provides an increase in signal to noise over analog integration for dim signals[21], which are common with *in vivo* two-photon calcium imaging data. A digital acquisition board (PCIe-6353, National Instruments) generated mirror command signals, and frame synchronization signals for the PMS-400A. Custom LabVIEW (National Instruments) software coordinated scan mirror drive signals, controlled the steering mirrors, communicated with the PMS-400A, and organized photon counting data into images.

The quality of the microscope's point spread function (PSF is crucial to the efficiency of two-photon excitation and ultimately image quality. We tested performance using a commercially available objective with a 0.80 NA (Nikon, CFI75 16x), which can provide a small PSF. Performance is expected to be excellent on axis, but can degrade at large scan angles due to aberrations in the scanning system. We evaluated the performance of the Trepan2p microscope by measuring the off-axis excitation volume as the full-width at half-maximum (FWHM) of the intensity profile obtained by imaging 0.2 µm beads (**SI Fig. 3a**). Radial FWHM was ~0.7 µm both on-axis and at the edges of the FOV in *Y*. At the edges in *X*, the *X* profile FWHM was 1.3 ± 0.1 µm. The axial FWHM was 5.4 ± 0.3 µm, which compares favorably with other two-photon microscopes[22,23]. The high performance objective and the corrected relay lens systems also lead to a FOV that shifted less than 35 µm at the edges (**SI Fig. 3b**). The asymmetry in the *X* and *Y* directions in the field is likely due to residual aberrations of the *X* to *Y* galvanometer scanner relay system

bioRxiv preprint doi: https://doi.org/10.1101/011320; this version posted November 12, 2014. The copyright holder for this preprint (which was not certified by peer review) is the author/funder. All rights reserved. No reuse allowed without permission.

(**SI Fig. 1**). This is within the range of *Z*-axis focusing of the individual imaging pathways.

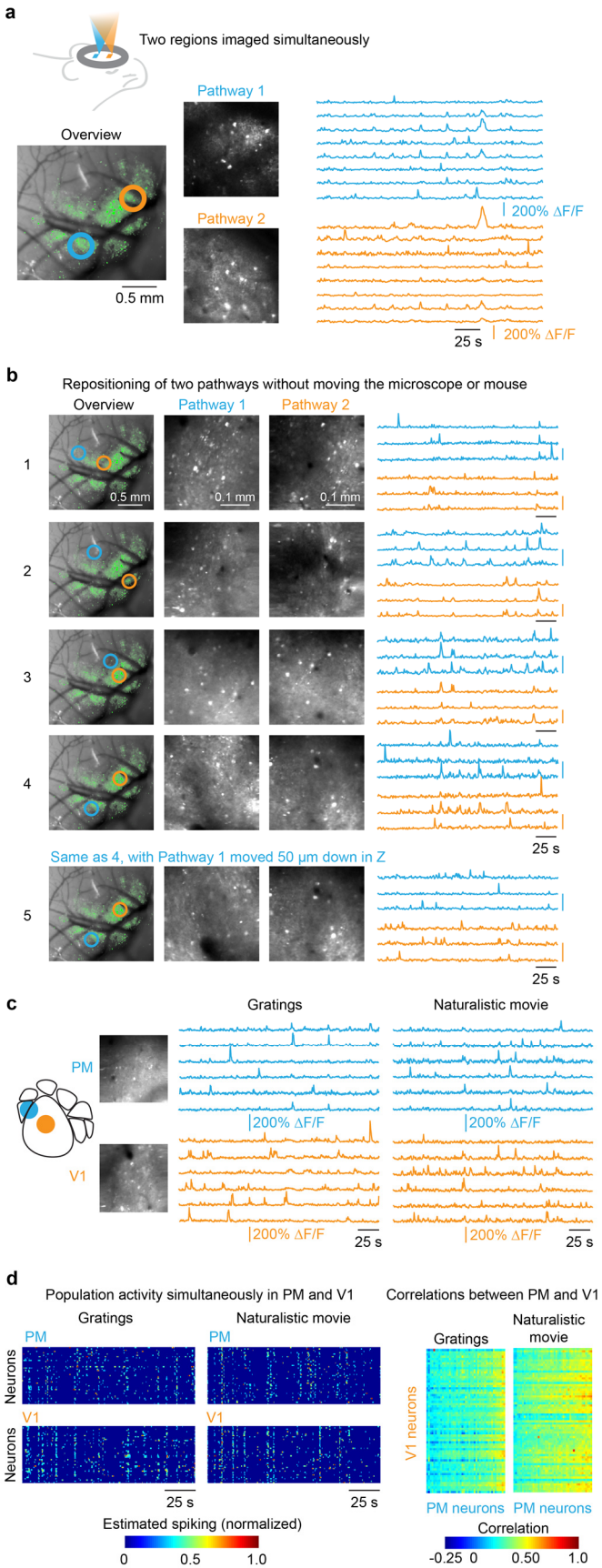

To demonstrate the functionality and flexibility of the Trepan2p, we performed two sets of imaging experiments. In the first experiment, we demonstrate operational Mode 1: large FOV imaging. To visualize multiple HVAs in one FOV, we first mapped retinotopy using intrinsic signal optical imaging[24] (**Fig. 2a**). Using the vasculature as landmarks, we then imaged spontaneous activity in a large cortical region of a mouse injected with AAV expressing GCaMP6s that included parts of four HVAs and V1 (**Fig. 2b**). This mode allowed for a wide FOV (1024 x 512 pixels over a square scanning region, 0.17 frames/s or 0.52 frames/s) while maintaining cellular resolution (**Fig. 2c**). Cells can clearly be identified throughout the entire FOV (1066 neurons detected, **Fig. 2d**) and Ca^{2+} signals are detected with high fidelity (**Fig. 2e**).

In Mode 2, both imaging pathways are utilized to image two smaller ROIs at higher frame rates simultaneously (256 x 256 pixels; 1.4 – 10 frames/s). Within the large FOV, the two imaging regions are determined by the deflection angles (Ω_1, Ω_2) imparted by the steering mirrors (SM1, SM2; **Fig. 1d**). This allows for spatial separation, yet simultaneous acquisition (**Fig. 3a**). Because the solid angle offsets (Ω_1, Ω_2) are not static and the mirrors are motorized, one can easily move the imaging regions to any position without moving the microscope or mouse (**Fig. 3b**). Additionally, the focal plane (*Z*) of each pathway can be controlled independently, allowing for imaging two different depths (compare configurations 4 & 5 in **Fig. 3b**). Furthermore, the two beam pathways each provide sufficient power (127 mW out of the objective for each pathway) and efficiency to image through cranial windows (**Figs. 2,3**). The fact that our design ultimately converges the two imaging streams back into a single objective is essential as it provides compatibility with standard sensory stimulus and behavior apparatus. While presenting visual stimuli to the mouse (gratings and naturalistic), we simultaneously recorded activity in V1 and the HVA PM (**Fig. 3d**). Estimated spiking was calculated following deconvolution of ΔF/F traces[13,25].

Figure 3. Twin region two-photon calcium imaging with independently positionable multiplexed pathways. (a) Two pathways imaged separate cortical regions simultaneously. **(b)** Within the same session, without moving the mouse or the microscope, the two pathways were moved to various configurations to image neuronal activity. In configuration 5, Pathway 2 was not changed from configuration 4, and Pathway 1 was moved in Z, not in X or Y. **(c)** Neuronal activity was imaged in two cortical areas, V1 and area PM, simultaneously. Visual stimuli, either drifting gratings or a naturalistic movie, were used to evoke activity. **(d)** Ca^{2+} signals were deconvolved to obtain spike rate estimates and examine correlations. **(e)** Correlations in activity were measured between pairs of cells, each pair consisting of a V1 neuron and an area PM neuron. These correlations were higher during presentation of the naturalistic movie compared to those during the drifting gratings. (The columns were ordered from low to high average correlation for presentation clarity.)

bioRxiv preprint doi: https://doi.org/10.1101/011320; this version posted November 12, 2014. The copyright holder for this preprint (which was not certified by peer review) is the author/funder. All rights reserved. No reuse allowed without permission.

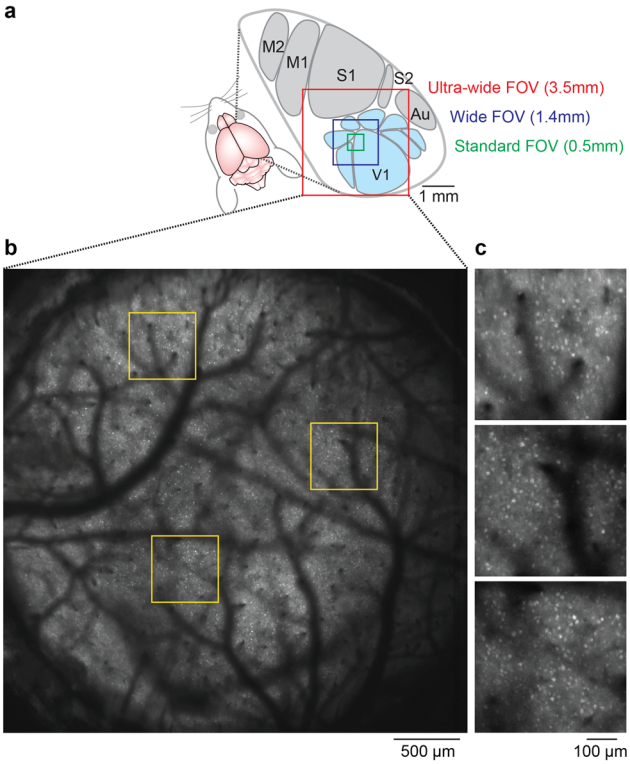

Figure 4. Further expansion of the FOV. (a) Anatomical layout of the mouse cortex with the FOV overlaid for the standard, and the wide and ultra-wide FOV presented in this work. **(b)** With the custom objective, the FOV is 3.5 mm. Within this FOV individual cells can be seen throughout (>5000 cell bodies are identified). **(c)** Zoom in of the green regions from (b). Cellular resolution in maintained even with the greatly expanded FOV.

Pairwise correlations between V1 and PM revealed an increase in correlated activity when the naturalistic movie is presented, compared to gratings (**Fig. 3d**). Such cross-area correlation analysis between densely sampled populations of neurons would not have been possible without the ability to image two cortical regions simultaneously.

Further expansion of the FOV

The successful neuroscience experiment demonstrated that all optical subsystems of the Trepan2p were functional. Next, we focused on the FOV itself and sought a further expansion. To further increase the FOV, we engineered additional improvements to the relay and scan optics to minimize aberrations to achieve or approach diffraction limited performance out to the desired scan angles. We employed optical design software (Zemax LLC) to optimize a multi-element relay lens system using commercial off the shelf (COTS) lenses. Additionally, we designed a scan and tube system from COTS components. Together these relay and scan multi-element systems allow us to scan at an angle of up to ~±18 degrees. With the new optical elements and the Nikon 16x objective, we have a FOV of 1.9 mm; we do, however, see vignetting beyond ~1.8 mm. This is most likely due to clipping within the objective.

To overcome the limitations of the commercial objective, and to push the FOV to even larger areas, we designed a custom objective using COTS components. The custom objective achieved an effective focal length of 30 mm and FOV of ~3.5 mm (NA ~ 0.38). At this scale, the entire visual cortex (including HVAs) as well as additional cortical structures could fit within the FOV (**Fig. 4a**). The improved system exhibited cellular resolution across the entire 3.5 mm FOV (**Fig. 4b**) and could clearly resolve cell bodies (**Fig. 4c**). Within this FOV >5,000 cells were identified.

DISCUSSION

We have demonstrated the Trepan2p microscope, which offers a wide FOV and two independent imaging beams for measuring activity in two spatially separated cortical areas simultaneously. This approach has several key advantages. First, the wide FOV offers overview imaging of extended cortical networks. Since the excitation volume is preserved across the FOV, the system provides access to ~7 to 50-fold more spatial information than a conventional 2p microscope. Second, the two imaging pathways allow for simultaneous imaging of spatially distinct areas. Third, the Trepan2p is flexible since the imaging beams can be re-positioned at will during imaging. The two imaging regions can be positioned anywhere within the larger FOV simply by moving the motorized steering mirrors. This allows an experimenter, within a single imaging session on an animal, to image multiple combinations of extended networks (**Fig. 3b**). Furthermore, the experimenter can independently position the two regions at different depths. The regions can be as large or small as needed for the experiment. For large overview imaging with two depths, both paths can be set to the maximum FOV and different imaging depths. Alternatively, to image the full FOV faster, two regions can be set to scan complementary halves of the FOV[17].

The Trepan2p requires only a single microscope objective, and this allows for flexible placement of sensory stimulation and behavior apparatus around the subject. Additionally, the working distance (≥3 mm) ensures that the system is compatible with simultaneous electrophysiology, and head-fixed behavior experiments. Overall, the microscope only occupies slightly more space than a traditional microscope (due to the delay path), and is simple to operate. The single set of galvanometer scanners, objective, and PMT keeps the cost approximately the same as a traditional two-photon microscope.

The system can be extended in several ways. First, the number of beams can be extended, as long as the interval between any laser pulses (across all multiplexed beams) is longer than the fluorescence lifetime of the fluorophore imaged[17,18]. Second, spatially patterned optogenetic stimulation can be applied through the wide field of view

bioRxiv preprint doi: https://doi.org/10.1101/011320; this version posted November 12, 2014. The copyright holder for this preprint (which was not certified by peer review) is the author/funder. All rights reserved. No reuse allowed without permission.

objective, using a dichroic mirror before the filters and PMT on the detection arm of the scope. Optogenetic stimulation can be applied in any pattern across the entire field of view, even if calcium imaging is only targeted to two specific areas. To simultaneously image multiple cortical regions that are beyond the FOV, or to access subcortical brain regions, the Trepan2p can be used in conjunction with microendoscopes[26-28]. Lateral views of the full cortical depth can be obtained using implanted microprisms[29,30] with the system. As we have shown, longer focal length and lower NA objectives are an exciting possibility to extend the FOV. Removing the restriction of using COTS components (designing custom lenses) will allow us to have diffraction or near diffraction limited performance across all scan angles. Also, custom designed objectives have the advantage of optimizing around a smaller excitation wavelength and limiting the vignetting (internal clipping) at large scan angles.

The Trepan2p provides systems neuroscience with a flexible way to image cellular-level neuronal activity not only across multiple cortical areas, but also over any model system that extends beyond the spatial limits of conventional two-photon microscopy. This approach enables measurements of neural activity correlations and dynamics across extended cortical circuitry with cellular resolution.

METHODS

Animals. All procedures involving living animals were carried out in accordance with the guidelines and regulations of the US Department of Health and Human Services and approved by the Institutional Animal Care and Use Committee at University of North Carolina. C57Bl/6 mice were housed under a reversed 12hr-light/12hr-dark light cycle with ad libitum access to food and water.

Viral injections. Adeno-associated virus (AAV) particles packaged and titered by Penn Vector Core (~10^{12} infectious units per ml; University of Pennsylvania, Philadelphia) were used to overexpress a genetically encoded calcium indicator, GCaMP6s (AAV1.Syn.GCaMP6s.WPRE.SV40 or AAV1.Syn-Lck-GCaMP6s.WPRE.SV40 from UNC Vector Core). ISOI was performed transcranially, and targeted burr holes were made for virus injections. A 4-mm wide full craniotomy and optical window installation (Fig. 2, 3) were carried out 4-6 weeks post injection. Carprofen (4.4 mg per kg body weight, s.c.) was given postoperatively before returning the animals to their cage.

Intrinsic signal optical imaging (ISOI). Custom instrumentation was adapted from the work of Kalatsky and Stryker[24]. Briefly, two F-mount lenses with respective focal lengths of 135 and 50 mm (Nikon) formed a tandem lens macroscope, which was attached to Dalsa 1M30 CCD camera (Teledyne DALSA). This configuration provided a 4.6 mm x 4.6 mm field of view (21.2 mm^2). Acquired images were binned 2 x 2 spatially, resulting in a final pixel size of 9.2 µm x 9.2 µm. The pial vasculature was illuminated through a green filter (550 ± 50 nm, Edmund Optics) and the vasculature map was captured through a second green filter (560 ± 5 nm). From the pial surface, the macroscope was then focused down 600 µm where intrinsic signals were illuminated with halogen light (Asahi Spectra) delivered via light guides and focusing probes (Oriel) through a red filter (700 ± 38 nm, Chroma). Reflected light was captured through a second red filter (700 ± 5 nm, Edmund Optics) at the rate of 30 frames per second with custom-made image acquisition software (adapted from code kindly provided by Dr. David Ferster, Northwestern University). Mice were head-fixed 20 cm from a flat 60 cm x 34 cm (width x height) monitor which was tilted towards the mouse 17.5° from vertical with their head angled to their right to cover the visual field (110° by 75°) of the contralateral eye. A light anesthetic plane was maintained with 0.5% isoflurane during imaging, augmented with acepromazine (1.5 - 3mg/kg), and the body temperature was kept at 37°C using feedback-controlled electric heat pad systems (custom-built).

Visual stimuli. A drifting white bar on a black background (elevation and azimuth direction; 3° thick) was used to map retinotopy during ISOI. These were produced and presented using MATLAB and the Psychophysics Toolbox[31,32]. A corrective distortion was applied to compensate for the flatness of the monitor[33] (code is available online, http://labrigger.com/blog/2012/03/06/mouse-visual-stim/). During calcium imaging, drifting gratings (0.04 cycles/°, 2 Hz, 8 directions, 10 s /direction, 10 s interstimulus interval) and a naturalistic movie were displayed on a small video display located 10 cm from the left eye. Light from the display was shielded from the imaging apparatus using a shroud over the monitor. The naturalistic movie was from a helmet-mounted camera during a mountain biking run. This movie, while not something a mouse would typically encounter, provided a visual stimulus with a large amount of optic flow.

Image analysis. Retinotopic maps were used to locate V1 and HVAs. Borders between these areas were drawn at the meridian of elevation and azimuth retinotopy. Magnitude response maps for patched gratings were also consulted for reconfirmation. Ca^{2+} signals were analyzed using custom software in MATLAB (Mathworks). Neurons were identified and segmented using either a pixel-wise correlation map[13] or a pixel-wise kurtosis map. The maps were segmented into individual ROIs (neurons and processes) and ΔF/F traces were calculated from the raw, unfiltered traces. For the correlation analysis, the ΔF/F traces were deconvolved prior to computing correlations[13].

Statistical analysis. Custom software for Igor Pro (Wavemetrics) and MATLAB (MathWorks) were used for statistical analysis.

Optical simulations. Relay, scan, tube, and objective lens systems were modeled in OpticStudio (Zemax, LLC).

bioRxiv preprint doi: https://doi.org/10.1101/011320; this version posted November 12, 2014. The copyright holder for this preprint (which was not certified by peer review) is the author/funder. All rights reserved. No reuse allowed without permission.

Excitation volume and field curvature measurements To calculate the excitation volume profiles for the Nikon 16x objective, image stacks ($\Delta Z = 0.4$ µm) were acquired of 0.2 µm beads (Invitrogen). High magnification images (0.17 µm/pixel) were acquired across the FOV. These same beads were imaged on and off axis to calculate overall field curvature of the imaging plane.

ACKNOWLEDGEMENTS

We are grateful to Kei Eto who kindly provided several mice for imaging, and Zemax LLC which provided upgraded software. This work was supported by the following: the National Institute of Child Health and Human Development (T32-HD40127 to J.N.S.); a Helen Lyng White Fellowship (I.T.S.); and a Career Development Award from the Human Frontier Science Program (00063/2012), and grants from the National Science Foundation (1450824) and the Whitehall Foundation (S.L.S.).

AUTHOR CONTRIBUTIONS

S.L.S. conceived and designed the Trepan2p imaging system. J.N.S. and S.L.S. engineered the system. J.N.S. developed the demultiplexing electronics, optimized the optical systems, wrote the software, and built the system. M.K. and J.N.S. modeled optical subsystems and M.K. consulted on optical optimizations. J.N.S., I.T.S., and S.L.S. performed the animal experiments. J.N.S. and S.L.S. analyzed and interpreted the data. J.N.S. and S.L.S. wrote the manuscript with input from all authors. I.T.S. and S.L.S. supervised the project.

REFERENCES

1. Denk, W., Strickler, J.H. & Webb, W.W. Two-photon laser scanning fluorescence microscopy. *Science* **248**, 73-6 (1990).
2. Stosiek, C., Garaschuk, O., Holthoff, K. & Konnerth, A. In vivo two-photon calcium imaging of neuronal networks. *Proc Natl Acad Sci U S A* **100**, 7319-24 (2003).
3. Chen, T.W. *et al.* Ultrasensitive fluorescent proteins for imaging neuronal activity. *Nature* **499**, 295-300 (2013).
4. Nimmerjahn, A., Mukamel, E.A. & Schnitzer, M.J. Motor behavior activates Bergmann glial networks. *Neuron* **62**, 400-12 (2009).
5. Dombeck, D.A., Harvey, C.D., Tian, L., Looger, L.L. & Tank, D.W. Functional imaging of hippocampal place cells at cellular resolution during virtual navigation. *Nat Neurosci* **13**, 1433-40 (2010).
6. Ohki, K., Chung, S., Ch'ng, Y.H., Kara, P. & Reid, R.C. Functional imaging with cellular resolution reveals precise micro-architecture in visual cortex. *Nature* **433**, 597-603 (2005).
7. Xu, N.L. *et al.* Nonlinear dendritic integration of sensory and motor input during an active sensing task. *Nature* **492**, 247-51 (2012).
8. Komiyama, T. *et al.* Learning-related fine-scale specificity imaged in motor cortex circuits of behaving mice. *Nature* **464**, 1182-6 (2010).
9. Harvey, C.D., Coen, P. & Tank, D.W. Choice-specific sequences in parietal cortex during a virtual-navigation decision task. *Nature* **484**, 62-8 (2012).
10. Jia, H., Rochefort, N.L., Chen, X. & Konnerth, A. Dendritic organization of sensory input to cortical neurons in vivo. *Nature* **464**, 1307-12 (2010).
11. Glickfeld, L.L., Andermann, M.L., Bonin, V. & Reid, R.C. Cortico-cortical projections in mouse visual cortex are functionally target specific. *Nat Neurosci* **16**, 219-26 (2013).
12. Theer, P., Hasan, M.T. & Denk, W. Two-photon imaging to a depth of 1000 microm in living brains by use of a Ti:Al2O3 regenerative amplifier. *Opt Lett* **28**, 1022-4 (2003).
13. Smith, S.L. & Hausser, M. Parallel processing of visual space by neighboring neurons in mouse visual cortex. *Nat Neurosci* **13**, 1144-9 (2010).
14. Dombeck, D.A., Khabbaz, A.N., Collman, F., Adelman, T.L. & Tank, D.W. Imaging large-scale neural activity with cellular resolution in awake, mobile mice. *Neuron* **56**, 43-57 (2007).
15. Wang, Q. & Burkhalter, A. Area map of mouse visual cortex. *J Comp Neurol* **502**, 339-57 (2007).
16. Tsai, P.S. & Kleinfeld, D. In vivo two-photon laser scanning microscopy with concurrent plasma-mediated ablation. in *Methods for In Vivo Optical Imaging*, Vol. 3 (ed. Frostig, R.) 59-115 (CRC Press, 2009).
17. Cheng, A., Goncalves, J.T., Golshani, P., Arisaka, K. & Portera-Cailliau, C. Simultaneous two-photon calcium imaging at different depths with spatiotemporal multiplexing. *Nat Methods* **8**, 139-42 (2011).
18. Amir, W. *et al.* Simultaneous imaging of multiple focal planes using a two-photon scanning microscope. *Opt Lett* **32**, 1731-3 (2007).
19. Grewe, B.F., Voigt, F.F., van 't Hoff, M. & Helmchen, F. Fast two-layer two-photon imaging of neuronal cell populations using an electrically tunable lens. *Biomed Opt Express* **2**, 2035-46 (2011).
20. Zinter, J.P. & Levene, M.J. Maximizing fluorescence collection efficiency in multiphoton microscopy. *Opt Express* **19**, 15348-62 (2011).
21. Driscoll, J.D. *et al.* Photon counting, censor corrections, and lifetime imaging for improved detection in two-photon microscopy. *J Neurophysiol* **105**, 3106-13 (2011).
22. Kobat, D., Horton, N.G. & Xu, C. In vivo two-photon microscopy to 1.6-mm depth in mouse cortex. *J Biomed Opt* **16**, 106014 (2011).
23. Ji, N., Sato, T.R. & Betzig, E. Characterization and adaptive optical correction of aberrations during in vivo imaging in the mouse cortex. *Proc Natl Acad Sci U S A* **109**, 22-7 (2012).
24. Kalatsky, V.A. & Stryker, M.P. New paradigm for optical imaging: temporally encoded maps of intrinsic signal. *Neuron* **38**, 529-45 (2003).
25. Yaksi, E. & Friedrich, R.W. Reconstruction of firing rate changes across neuronal populations by temporally deconvolved Ca2+ imaging. *Nat Methods* **3**, 377-83 (2006).
26. Jung, J.C., Mehta, A.D., Aksay, E., Stepnoski, R. & Schnitzer, M.J. In vivo mammalian brain imaging using one- and two-photon fluorescence microendoscopy. *J Neurophysiol* **92**, 3121-33 (2004).
27. Barretto, R.P. & Schnitzer, M.J. In vivo optical microendoscopy for imaging cells lying deep within live tissue. *Cold Spring Harb Protoc* **2012**, 1029-34 (2012).
28. Ziv, Y. *et al.* Long-term dynamics of CA1 hippocampal place codes. *Nat Neurosci* **16**, 264-6 (2013).
29. Chia, T.H. & Levene, M.J. Microprisms for in vivo multilayer cortical imaging. *J Neurophysiol* **102**, 1310-4 (2009).
30. Andermann, M.L. *et al.* Chronic cellular imaging of entire cortical columns in awake mice using microprisms. *Neuron* **80**, 900-13 (2013).
31. Brainard, D.H. The Psychophysics Toolbox. *Spat Vis* **10**, 433-6 (1997).
32. Pelli, D.G. The VideoToolbox software for visual psychophysics: transforming numbers into movies. *Spat Vis* **10**, 437-42 (1997).
33. Marshel, J.H., Garrett, M.E., Nauhaus, I. & Callaway, E.M. Functional specialization of seven mouse visual cortical areas. *Neuron* **72**, 1040-54 (2011).